Arab J Geosci (2013) 6:1447–1456
DOI 10.1007/s12517-011-0453-x

ORIGINAL PAPER

The application of lithogeochemical and alteration index for copper mineralization in the Sonajil area, NW Iran

Kaveh Pazand · Ardeshir Hezarkhani · Mohammad Ataei

Received: 26 June 2011 / Accepted: 19 October 2011 / Published online: 16 November 2011

Abstract The Sonajil intrusive is located about 60 km southeast of Ahar, in Azarbaijan province in northwestern Iran, and is intruded into by andesitic trachytic Eocene pyroclastics and agglomerate. To the center, the stock is hydrothermally altered, that contains sub-economic copper mineralization. The 1,248 cells with 100×100 m grid were sampled, and measurement of elements by ICP-MS method and major oxides included by X-ray fluorescence method was performed. After statistical interpretations, geochemical anomalies and indices alteration (sericitization, alkali, Spitz–Darling, chloritization, Hashimoto, Hashiguchi) were calculated, and their map distribution was prepared. Based on these maps and other interpretations of data, our study indicated that despite the anomaly of copper and other elements such as gold, molybdenum, lead, arsenic and antimony of not being quite consistent, almost all of them are within the alteration zones.

Keywords Sonajil · Lithogeochemical · Indices alteration · Anomaly · Copper

K. Pazand (✉)
Science and Research Branch,
Department of Mining Engineering, Islamic Azad University,
Tehran, Iran
e-mail: kaveh.pazand@gmail.com

A. Hezarkhani
Department of Mining, Metallurgy and Petroleum Engineering,
Amirkabir University,
Hafez Ave. No. 424,
Tehran, Iran

M. Ataei
Department of Mining, Geophysics and Petroleum Engineering,
Shahrood University of Technology,
7th tir Sq, PO Box 36155-316, Shahrood, Iran

Introduction

Lithogeochemical data, comprising both major oxide and trace elements, are frequently used in geological mapping and tectonic studies to classify rock types, identify chemical variations due to fractionation trends, and characterize tectonic environments. Lithogeochemical data are also useful for mineral exploration studies by providing chemical information on alteration and mineralization patterns. The ultimate goal of the statistical and spatial analysis of lithogeochemical data for mineral exploration is the detection of zones of elevated concentrations (e.g., geochemical anomalies) of oxide or trace elements that may be reflective of mineral deposits (Harris et al. 1999, 2000). One of the major improvements in mineral exploration has been the recognition of regional-scale alteration patterns in hydrothermal systems related to plutonic and volcanic environments (Franklin 1997; Hannington et al. 2003). Alteration indexes allow for more accurate mapping of hydrothermal alteration in rocks and have been instrumental in the discovery of many base and precious metal (especially Cu porphyry) ore deposits in both submarine and subaerial environments (Sillitoe 1995). In Iran, all known porphyry and skarn mineralization occurs in the Cenozoic Sahand-Bazman orogenic belt (Fig. 1). This belt was formed by subduction of the Arabian plate beneath central Iran during the Alpine orogeny (Berberian and King 1981; Pourhosseini 1981; Niazi and Asoudeh 1978) and hosts two major porphyry Cu deposits. The Sar-cheshmeh deposit contains 450 million tonnes of sulfide ore with an average grade of 1.13% Cu and 0.03% Mo (Waterman and Hamilton 1975; Hezarkhani 2006a). The Sungun deposit contains 500 million tonnes of sulfide reserves grading 0.76% Cu and 0.01% Mo (Hezarkhani and Williams-Jones 1998). A number of small and sub-economic porphyry copper deposits (for example Sonajil) are all associated with mid- to late-Miocene diorite/

granodiorite to quartz–monzonite stocks. Important Cu skarn deposits also are found in and around the Oligocene–Miocene volcanic rocks in this belt (Mollai et al. 2009; Hezarkhani 2006b; Mollai 2004, 2005, 2007). This area was already studied on 1:25,000 regional scales by stream sediment geochemical exploration phase and has shown significant geochemical anomalies of Cu (Kavoshgaran Co. 2007). Based on the results, the area was selected for lithogeochemical exploration survey. One of the questions raised is whether there is a relationship between copper mineralization and alteration in the region. This paper demonstrates the use of regional geochemical surveys for Cu exploration and local lithogeochemical for mapping alteration intensity and facies and to introduce diamond exploration methods, at the Sonajil Cu porphyry mineralization.

Geology setting

The Sonajil intrusive is located about 60 km southeast of Ahar, in Azarbaijan province in northwestern Iran (Fig. 1) and is intruded into by andesitic trachytic Eocene pyroclastics and agglomerate. To the center, the stock is hydrothermally altered that contains sub-economic copper mineralization (Hezarkhani 2008). The oldest rocks exposed in the study area are a 600-m sequence of Eocene with intercalations of andesite and andesitic breccias and a 1,500-m-thick sequence of Middle to early Late Tertiary, intermediate, calc-alkaline lavas, and tuffaceous rock, intruded by numerous calc-alkaline andesitic dykes (Fig. 1). The entire stock and volcanic cover rocks seem to be located within a caldera (Hezarkhani 2008). The intrusive rocks at Sonajil area mainly are (1) diorite/granodiorite, (2) quartz–monzonite/monzonite, and (3) andesitic and related dykes, in order of emplacement. The monzonite/quartz–monzonites are mainly porphyritic and exposed to the south of the stock, and intrude the monzonite/quartz–monzonite. The intrusive is generally unfoliated and porphyritic. Rocks in the study area were subjected to intense hydrothermal alteration, especially within and adjacent to the diorite/granodiorite intrusion. Even in the outermost part of the area, it is impossible to find completely fresh igneous rocks in outcrop. Several stages of weak hydrothermal alteration and associated poor mineralization have produced new minerals, created new textural relationships, and in many cases, obliterated the primary character of the rocks (Hezarkhani 2008).

Sampling and analysis

To design the sampling pattern, results of previous geochemical stream sediment and heavy mineral studies, a preliminary geological map, and field notes were used. To cover all of the area, grid cells 100×100 taking 1,248 lithogeochemical samples were used (Fig. 2). For each sample, at least 40 pieces of surface rock chip samples (100 g) were collected from 40 points randomly inside each cell, and minimum sample weight is 4 kg. Measurement of 44 elements (Ag, Al, As, Au, Ba, Be, Bi, Ca, Cd, Ce, Co, Cr, Cs, Cu, Fe, Hg, K, La, Li, Mg, Mn, Mo, Na, Nb, Ni, P, Pb, Rb, Re, S, Sb, Sc, Sn, Sr, Te, Th, Ti, Tl, U, V, W, Y, Zn, and Zr) by inductively coupled plasma-mass spectrometry method using natural rock standards as reference samples for calibration and major oxides that include MgO, Fe_2O_3, Al_2O_3, Na_2O, K_2O, CaO, and SiO_2 by X-ray fluorescence spectrometer method in the 1,248 rock samples was performed in AMDEL Australian laboratory. Appropriate standards and sample analytical duplicates were introduced in each sample batch at a rate of 5%. With the aim of providing the most real indices and indicators of individual constituents by use of statistical treatment of the analytical results, the minimum values are considered to be the amount represented by half of the values of the lower sensitivity limit of the corresponding chemical element (National Iranian Copper Industries 2008).

Fig. 1 Geology map of Iran (modified from Stoklin 1977; Shahabpour 1994) and detailed geological map of the Sonajil area showing the distribution of different igneous suites (modified from the geological map of Sonajil by the National Iranian Copper Industries Company-Exploration Department) ▶

Results

Geochemical characteristics of elements are summarized in Table 1, with the values for minimum, maximum, standard deviation (Std. Dev.), mean, range, kurtosis, and skewness. It should be noted that copper is highly enriched in the region, and its value varies from 7.10 to 21,200 ppm. Among polymetal elements such as Pb, Zn, Mo, Au, As, Ag, Ni, Co, and U, Cu concentration has the greatest range of variation with standard deviation equal to 956.49 (Table 1).

The concentration ranges for Cu and the other trace elements in the field are presented in Fig. 3. According to drawing diagrams in Fig. 3, values out of each category have been defined. Values outside the category of some elements are indicative of a particular phenomenon. For example, values outside of K denoted phyllic alteration and Al guidance for advanced argillic. For elements such as As, Au, Cu, Mo, Pb, Zn, and Sb, they indicate metal mineralization and local enrichment of these elements. This was about elements such as Ca, Na, Ti, and Zr which are due to differences in lithology in rock units region.

The copper, gold, arsenic, molybdenum, antimony, and zirconium distributions all show asymmetrical, positively

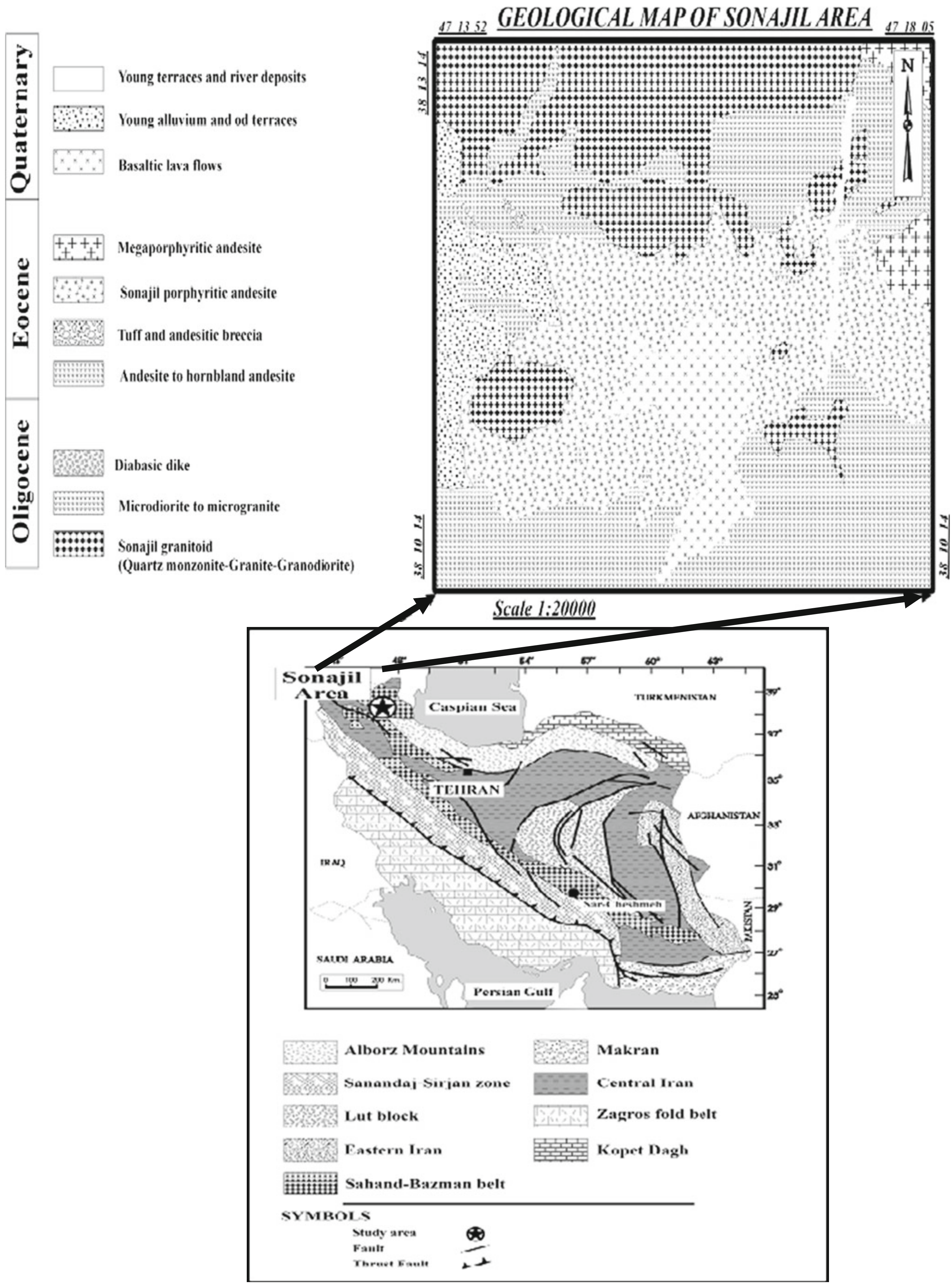
GEOLOGICAL MAP OF SONAJIL AREA
47 13 52
47 18 05
38 13 14
38 10 14
N
Scale 1:20000
Quaternary
Young terraces and river deposits
Young alluvium and od terraces
Basaltic lava flows
Eocene
Megaporphyritic andesite
Sonajil porphyritic andesite
Tuff and andesitic breccia
Andesite to hornbland andesite
Oligocene
Diabasic dike
Microdiorite to microgranite
Sonajil granitoid
(Quartz monzonite-Granite-Granodiorite)
Sonajil Area
Caspian Sea
TURKMENISTAN
TEHRAN
AFGHANISTAN
IRAQ
SAUDI ARABIA
Persian Gulf
PAKISTAN
Alborz Mountains
Sanandaj-Sirjan zone
Lut block
Eastern Iran
Sahand-Bazman belt
Makran
Central Iran
Zagros fold belt
Kopet Dagh
SYMBOLS
Study area
Fault
Thrust Fault

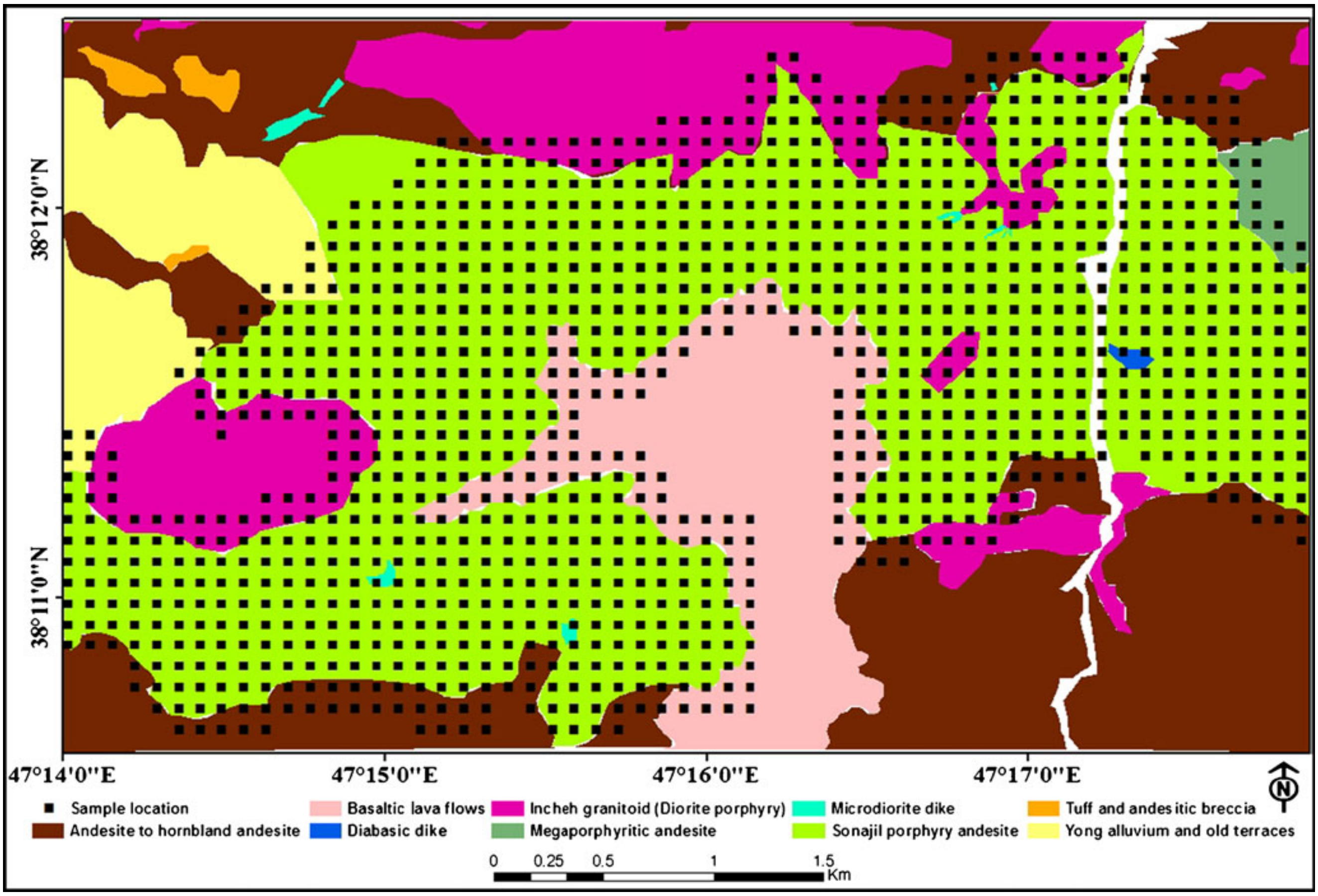

Fig. 2 Lithogeochemical sampling pattern location cells in the study area

skewed distribution patterns. Other elements in Fig. 3 showed slightly normal or symmetrical. There is no good correlation between copper and other metals. Most of the observed positive correlation between elements in the area was obtained by Mg–Co and Th–U with correlation coefficients equal to 0.8 and 0.82, respectively (Fig. 4). Between Cu and rock-forming elements such as K, Na, and Al, the constant correlation is seen, due to the lack of diversity in the rock of the study area.

Geochemical distribution

Distribution maps for several elements were prepared (Fig. 5) based on the kriging method (Panahi et al. 2004). The objective of the kriging is to provide a probability-based estimate of trace and heavy element distribution and their spatial distribution. High amounts of arsenic have a wide distribution in the north, northeast, and southwest parts of the region. Au is only in two points in the northeast, and limited areas in the southwest are seen as an anomaly. The highest amounts of Sb are located in the southeast region. The heterogeneous distributions of Pb and Zn are variable in all areas. Mo dispersion is greatest in the northeast, and in the southwestern area, it shows an anomaly, with fewer dispersions. Copper has isolated anomalies, and in scattered locations in the southwest, central, and northeast areas, it has an anomaly (Fig. 5).

Alteration

The rocks of the area have hydrothermal alteration (Hezarkhani 2008). Consequently, to find relationships between mineralization and alteration in the area, the two types of alteration maps were produced. The first series was based on the alteration indices (sericitization, chloritization, Spitz–Darling, and Hashimoto alteration index) and alterations obtained from aster data based on satellite images (phyllic, argillic, and iron oxide). Sericitization index (K_2O/(Na_2O+CaO)) (Kishida and Kerrich 1987) in two areas in the northeast and southwest has the largest range of their values (Fig. 6). The index distribution map of Spitz–Darling (Al_2O_3/Na_2O ratio) (Spitz and Darling 1978) shows an enrichment of Al_2O_3 rather Na_2O unit that refers to empty sodic in rocks of the region. High-grade area of this

Table 1 Summary of statistical parameters of element concentrations of samples from the Sonajil area

Element (ppm)	K	Au	Cr	Mn	Ni	Pb	Sr	Ba	Be	Ti	Fe	Al	La	Sc	Ca
N	1,248	1,248	1,248	1,248	1,248	1,248	1,248	1,248	1,248	1,248	1,248	1,248	1,248	1,248	1,248
Mean	23,442.29	24.39	15.70	650.37	14.31	20.02	746.29	927.12	1.62	3,874.82	38,855.25	83,377.50	31.43	8.55	23,331.50
Median	20,300.00	1.00	8.00	621.50	8.00	16.20	624.50	896.00	1.40	3,800.00	37,950.00	83,400.00	30.00	8.00	21,100.00
Std. deviation	13,401.48	283.48	17.45	405.69	14.45	18.53	462.20	312.57	0.78	1,111.98	13,503.62	15,035.67	12.82	3.93	17,660.31
Skewness	1.25	26.16	4.05	2.34	1.34	4.74	1.33	1.98	0.94	0.08	1.87	−0.01	0.51	1.00	1.20
Kurtosis	2.44	781.87	39.59	16.62	0.72	38.76	3.23	14.76	0.86	−0.34	11.11	2.71	1.09	1.33	4.86
Range	94,700.00	8.89	265.00	5,210.00	76.00	227.00	3,870.00	3,919.20	4.80	7,380.00	155,850.00	178,674.00	118.00	26.00	176,974.00
Minimum	0.00	0.00	0.00	0.00	0.00	0.00	0.00	0.80	0.00	10.00	150.00	326.00	0.00	0.00	26.00
Maximum	94,700.00	8.89	265.00	5,210.00	76.00	227.00	3,870.00	3,920.00	4.80	7,390.00	156,000.00	179,000.00	118.00	26.00	177,000.00
Element (ppm)	Li	P	V	Mg	Na	S	Zr	Hg	Ag	As	B	Bi	Co	Cu	Mo
N	1,248	1,248	1,248	1,248	1,248	1,248	1,248	1,248	1,248	1,248	1,248	1,248	1,248	1,248	1,248
Mean	24.42	1,500.44	113.53	8,939.81	21,654.65	1,450.30	98.29	0.02	0.60	57.53	0.00	0.15	10.96	240.58	4.73
Median	19.45	1,380.00	102.50	7,440.00	23,200.00	300.00	91.00	0.00	0.48	42.80	0.00	0.00	10.70	72.95	3.00
Std. deviation	19.13	673.48	52.52	6,710.24	11,349.22	3,745.57	59.54	0.06	0.47	59.52	0.00	0.40	6.40	956.49	6.85
Skewness	3.91	0.59	0.88	0.57	−0.27	6.00	0.98	3.98	2.64	4.45		5.72	0.38	12.30	10.05
Kurtosis	26.80	−0.53	0.95	−0.77	−1.04	47.09	1.80	19.62	10.77	42.71		40.70	−0.24	211.87	177.75
Range	249.00	3,012.00	349.00	29,075.00	45,100.00	47,500.00	382.00	0.57	3.48	896.00	0.00	4.40	37.60	21,192.90	150.70
Minimum	0.00	208.00	0.00	25.00	0.00	0.00	0.00	0.00	0.00	0.00	0.00	0.00	0.20	7.10	0.30
Maximum	249.00	3,220.00	349.00	29,100.00	45,100.00	47,500.00	382.00	0.57	3.48	896.00	0.00	4.40	37.80	21,200.00	151.00
Element (ppm)	Sb	Zn	Sn	W	Cs	Nb	U	Te	Cd	Rb	Th	Y	Ce	Tl	Re
N	1,248	1,248	1,248	1,248	1,248	1,248	1,248	1,248	1,248	1,248	1,248	1,248	1,248	1,248	1,248
Mean	9.74	73.07	1.13	3.31	3.83	13.03	2.16	0.25	0.11	64.27	7.63	10.80	53.36	0.37	0.00
Median	4.00	73.20	1.00	2.60	3.20	12.25	1.73	0.00	0.00	53.45	6.13	10.80	50.20	0.30	0.00
Std. deviation	16.49	41.82	0.60	2.72	3.27	6.01	1.32	0.72	0.16	48.88	5.09	4.49	23.39	0.41	0.01
Skewness	5.81	7.69	4.98	2.46	4.62	0.73	1.08	11.86	3.80	1.12	1.88	0.31	0.51	2.16	25.08
Kurtosis	68.36	148.25	60.99	9.91	56.92	0.36	0.99	234.47	29.69	1.18	7.53	0.18	−0.29	6.38	731.02
Range	285.00	938.00	11.00	25.10	56.30	36.60	8.95	16.70	2.10	284.60	47.87	25.89	129.90	2.80	0.24
Minimum	0.00	1.00	0.00	0.30	0.00	0.00	0.22	0.00	0.00	0.40	0.53	0.61	3.10	0.00	0.00
Maximum	285.00	939.00	11.00	25.40	56.30	36.60	9.17	16.70	2.10	285.00	48.40	26.50	133.00	2.80	0.24

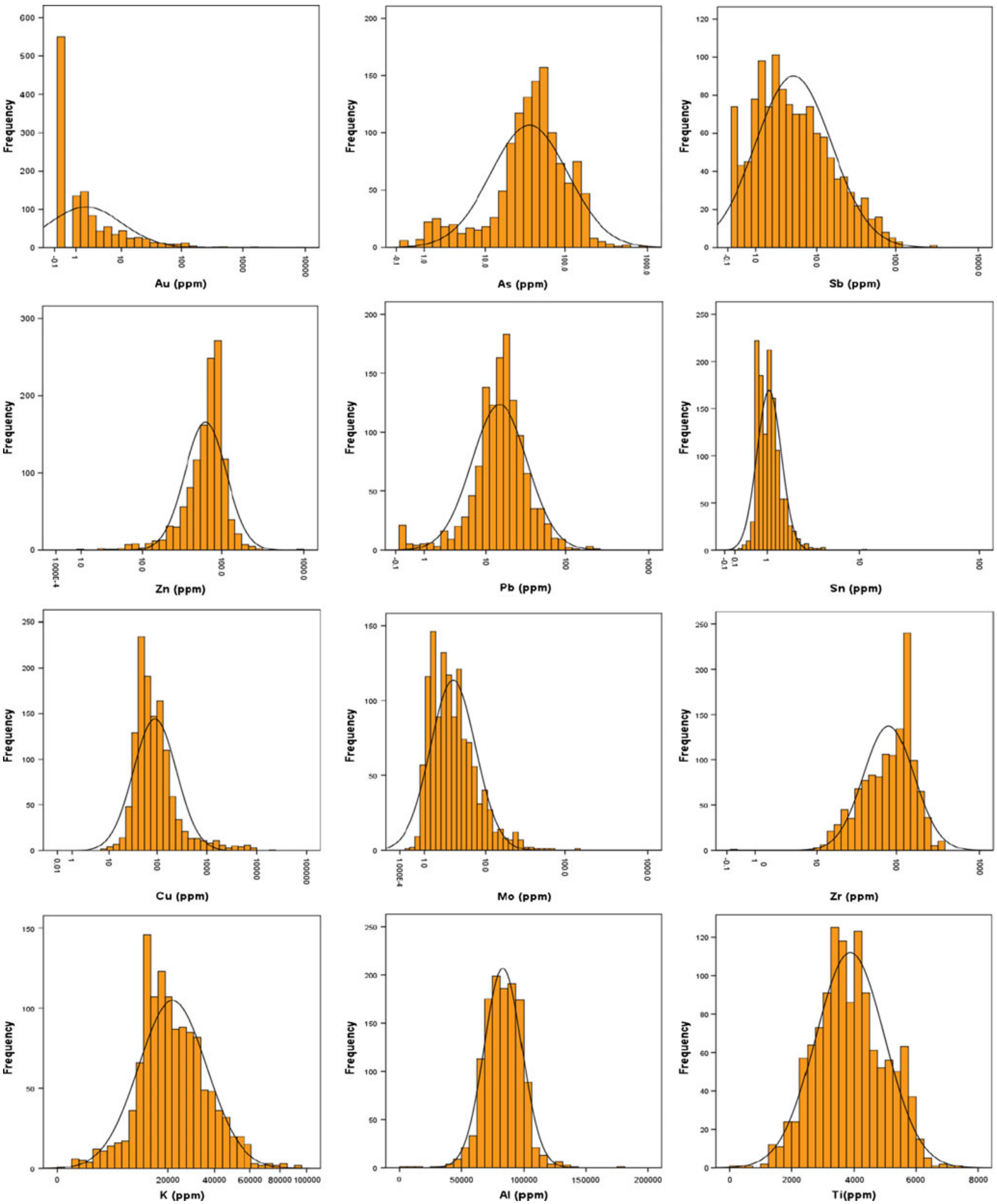

Fig. 3 Histograms of the elements in the Sonajil area

variable in the center, east, and southwest of the region is visible as small discrete areas. The Hashimoto index (Harris et al. 2000) distribution map that shows input of K and Mg and exit of Ca and Na confirms possible locations specified by mineralization $((MgO+K_2O)/(MgO+K_2O+CaO+Na_2O))$. This index is widely spread in the east and west

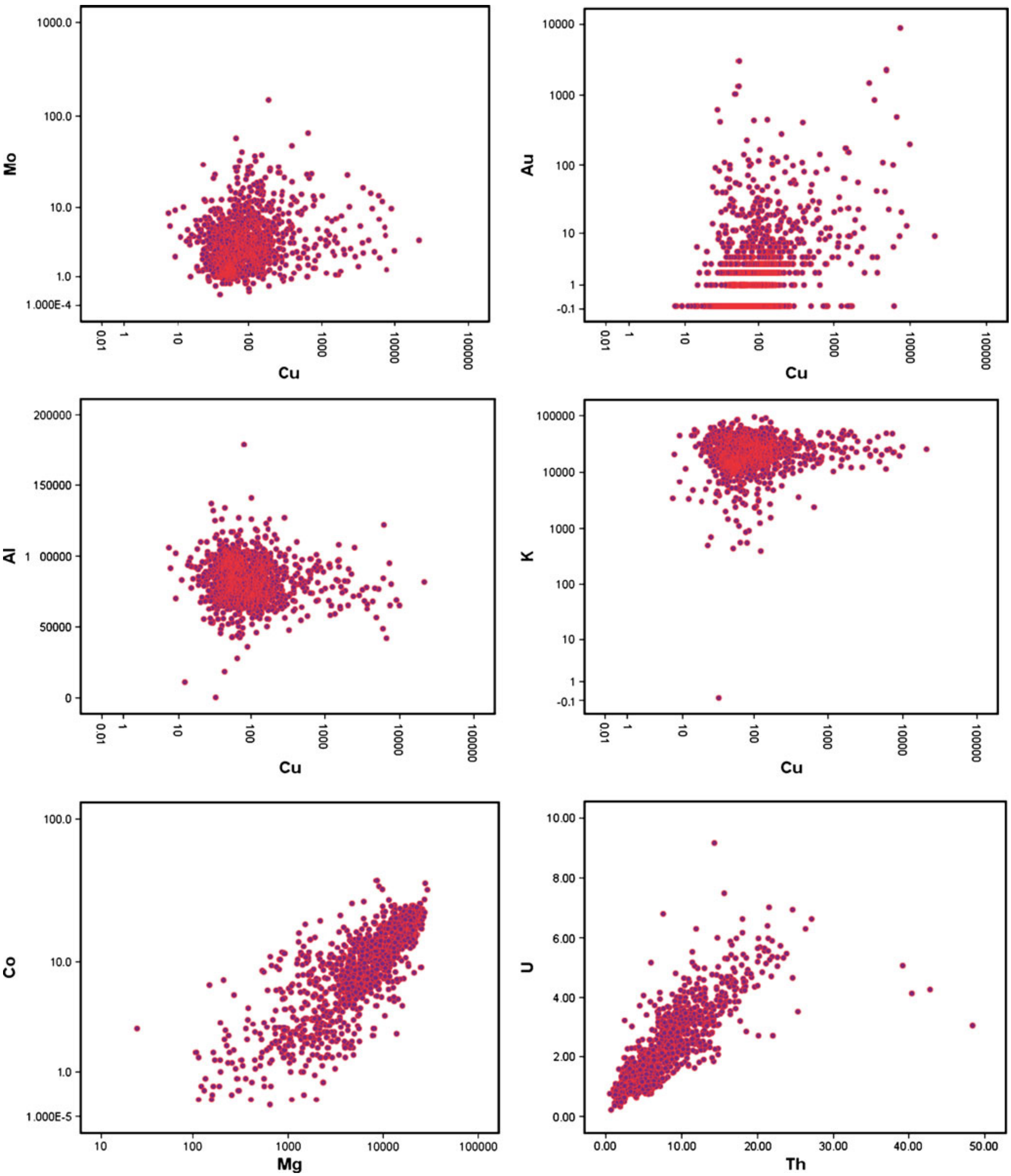

Fig. 4 Correlation between paired elements in the study area

regions and indicates that there is further potential of these areas for mineralization (Fig. 6). The index distribution map of chloritization (Yoshihiro 2009) has a high-grade area in the NE, SW, and central part of area. Remote sensing data (Aster data) were used for extraction of argillic, phyllic, and iron oxide alteration (Azizi et al. 2010) (Fig. 7).

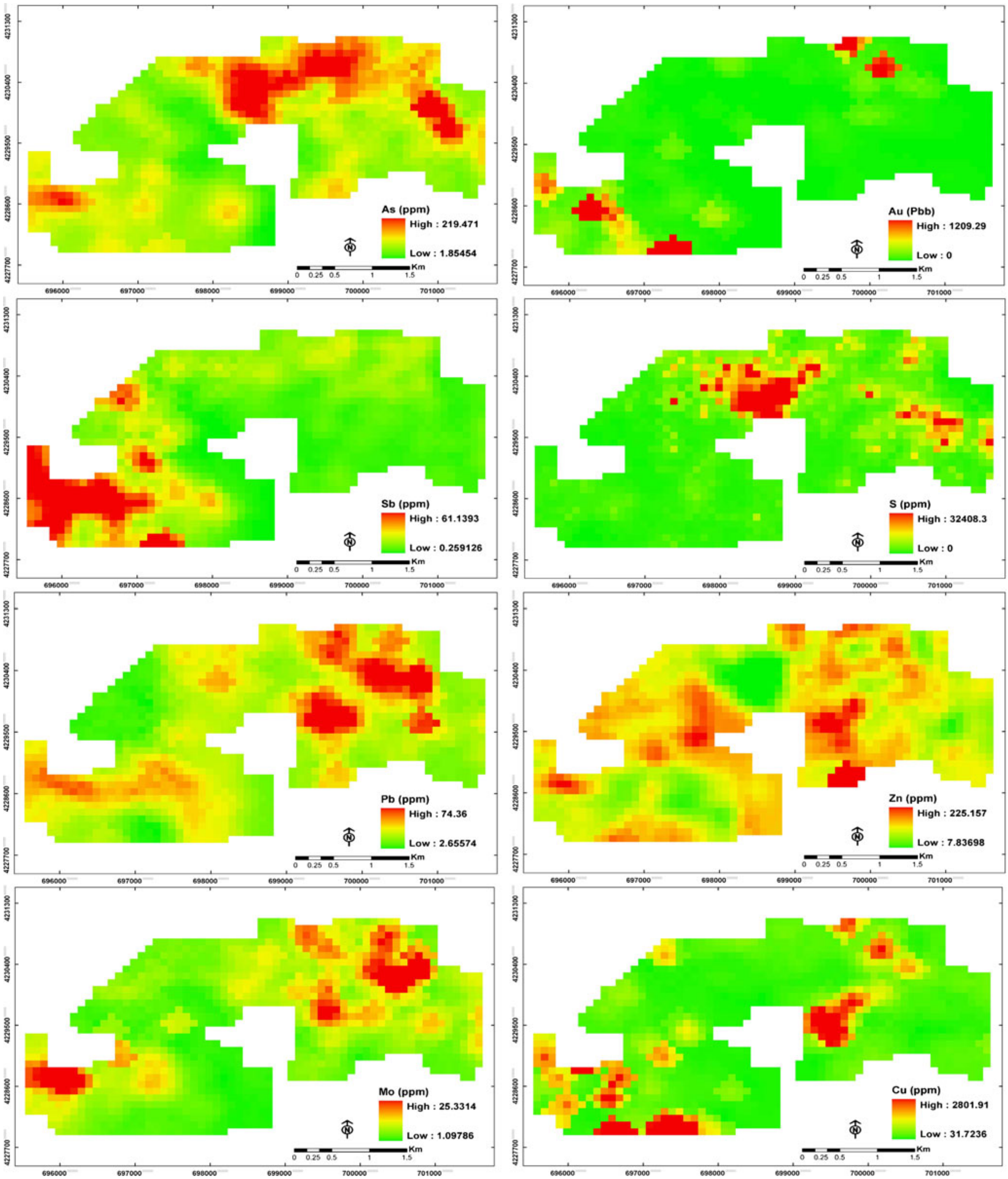

Fig. 5 Distribution maps for Au, As, Sb, S, Zn, Pb, Mo, and Cu element in study area

Conclusion

The relationship between alteration and mineralization has been documented by many researchers (Hezarkhani and Williams-Jones 1998; Angeles et al. 2008). By comparison of the anomalies of copper and other elements in the region with alteration indices and alteration halo, it becomes clear that despite the anomaly of copper and other elements such

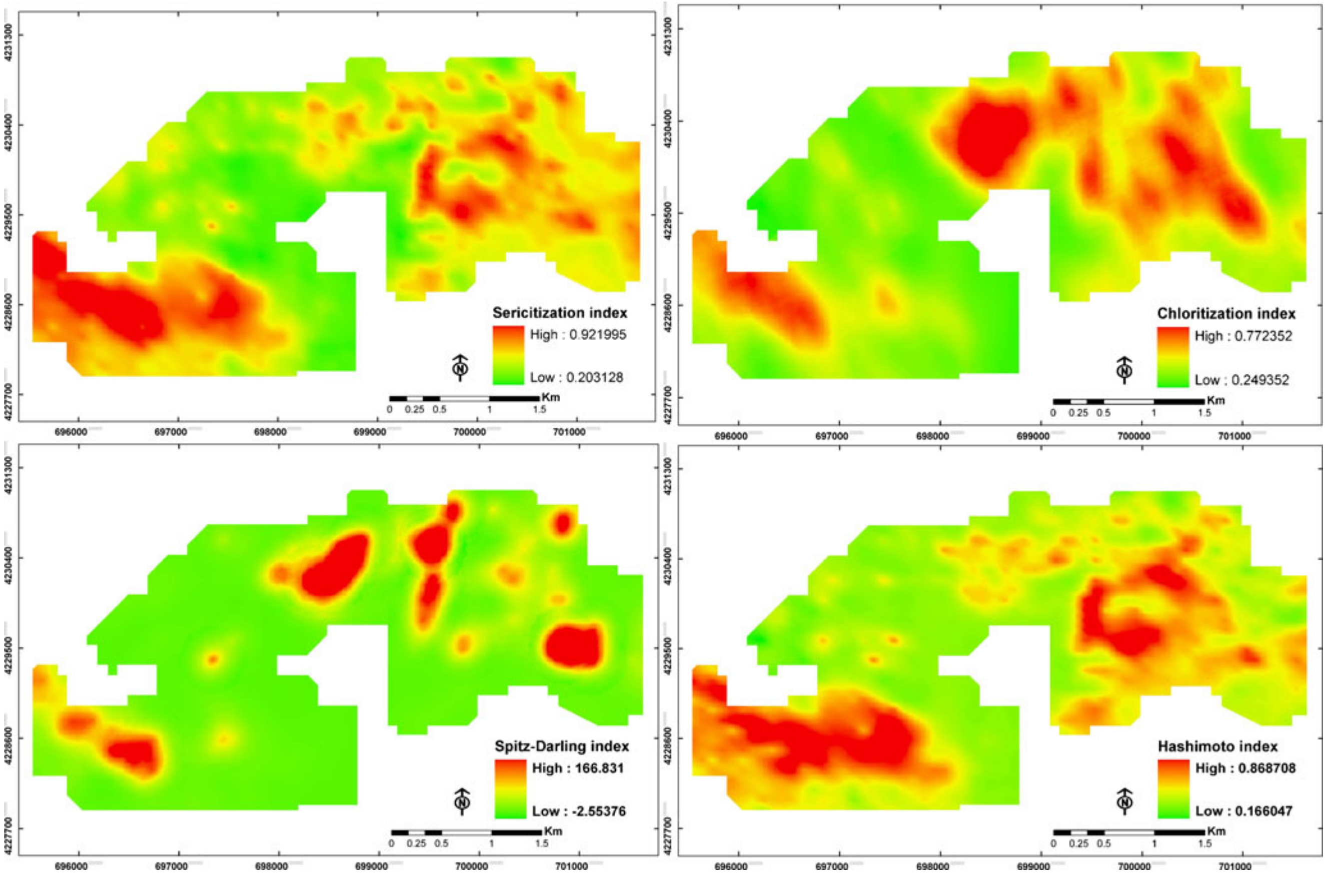

Fig. 6 Distribution map of sericitization, chloritization, Spitz–Darling, and Hashimoto alterations index

as gold, molybdenum, lead, arsenic, and antimony of not being quite consistent, almost all of them are within the alteration zones. This relationship in Sb, Zn, and Pb is less than the other elements. Also, mineralization associated with iron oxide alteration in this region is low. The results show that with high reliability, indicators and halo alteration can be used in copper and other metal explorations. This research has been done on a local area, and because of the large number of samples, it takes too much time and cost. The results show that there is a high relationship between copper mineralization and alteration in the area. According to the existence potential for copper mineralization in the Azerbaijani region, the results can be used in future exploration work in the region especially for areas in the regional exploration and polymetal mineralization.

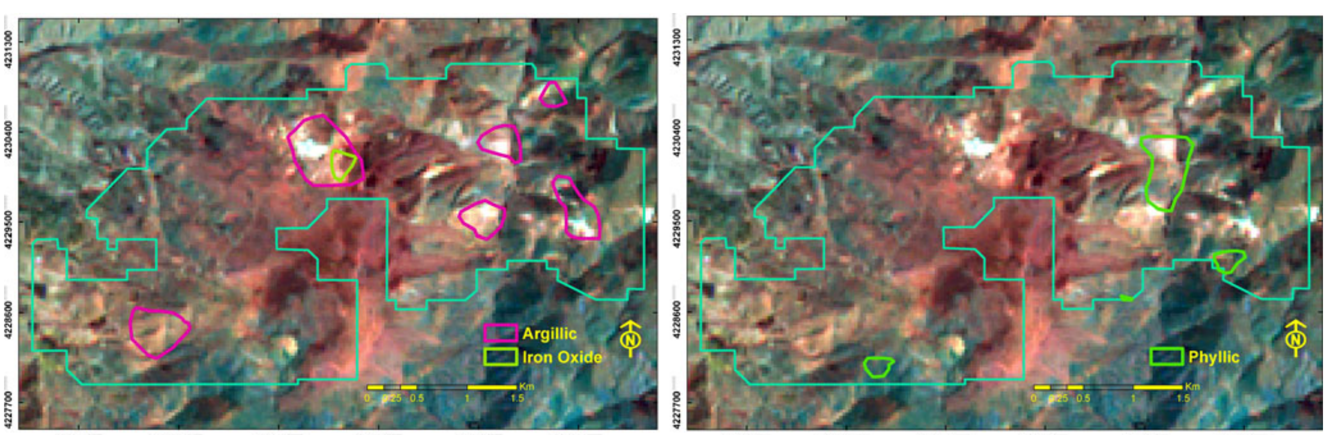

Fig. 7 Distribution map of phyllic, argillic, and iron oxide alteration in area

References

Angeles CA, Prihatmoko S, Walker J (2008) Geology and alteration-mineralization characteristics of the Cibaliung epithermal gold deposit, Banten, Indonesia. Resour Geol 52:329–339

Azizi H, Tarverdi M, Akbarpour A (2010) Extraction of hydrothermal alterations from ASTER SWIR data from east Zanjan, northern Iran. Adv Space Res 46:99–109

Berberian M, King GC (1981) Towards a paleogeography and tectonic evolution of Iran. Canadian Journal of Earth Sciences 18:210–265

Franklin JM (1997) Lithogeochemical and mineralogical methods for base metal and gold exploration. In Proceedings of Exploration 97, 4th Decennial International Conference on Mineral Exploration, Toronto, Ont., Sept. 14–18, 1997. pp. 191–208

Hannington MD, Santaguida F, Kjarsgaard IM, Cathles LM (2003) Regional-scale hydrothermal alteration in the Central Blake River Group, western Abitibi subprovince, Canada: implications for VMS prospectivity. Mineral ium Deposita 38:393–422

Harris JR, Wilkinson L, Grunsky EC, Heather K, Ayer J (1999) Techniques for analysis and visualization of lithogeochemical data with applications to the Swayze greenstone belt, Ontario. J Geochem Explor 67:301–334

Harris JR, Wilkinson L, Grunsky EC (2000) Effective use and interpretation of lithogeochemical data in regional mineral exploration programs: application of Geographic Information Systems GIS technology. Ore Geol Rev 16:107–114

Hezarkhani A (2006a) Geochemistry of the Anjerd Skarn and its association with copper mineralization, northwestern Iran. Int Geol Rev 48:892–909

Hezarkhani A (2006b) Petrology of the intrusive rocks within the Sungun Porphyry Copper Deposit, Azerbaijan, Iran. Journal of Asian Earth Sciences 27:326–340

Hezarkhani A (2008) Hydrothermal evolution in Sonajil porphyry copper system (East Azarbaijan Province, Iran): the history of an uneconomic deposit. Journal of IGR, Stanford, USA 50:483–500

Hezarkhani A, Williams-Jones AE (1998) Controls of alteration and mineralization in the Sungun porphyry copper deposit: evidence from fluid inclusions and stable isotopes. Econ Geol 93:651–670

Kavoshgaran Co (2007) Alteration survey report in Sonajil area. Copper Company, Internal Report, no. 2., P. 40

Kishida A, Kerrich R (1987) Hydrothermal alteration zoning and gold concentration at the Kerr-Addisin archean lode gold deposit,/ Kirkland lake,/ontarion. Econ Geol 82:649–690

Mollai H, Dave VKS, Sharma R (2004) Copper mineralization at Mazraeh NorthWest of Iran: evidences for fluid evolution and Skarn deposit. Abstract volume of the 32nd International Geological Congress. Florence, August 20–28, 2004, p. 223

Mollai H, Torshizian HA, Babakhani A (2005) Geology and petrological study of Cretaceous sequences in Gharah Dagh Formation, North West of Iran, with special reference to theMazraeh region. Abstracts Volume of the International Symposiumon the Cretaceous 5–9 Sept. 2005. University of Neuchatel, Switzerland, p 147

Mollai H, Sharifian RA, Darvishzadeh A (2007) Mineralogy and mineral chemistry of epidote in Mazraeh skarn deposit north of Ahar, Eastern Azarbaijan. Proceedings volume of the First Applied Geological Congress, 15–16 May 2007. Islamic Azad University, Mashhad Branch, Iran (in Farsi)

Mollai H, Sharma R, Pe-Piper G (2009) Copper mineralization around the Ahar batholith, north of Ahar (NW Iran): evidence for fluid evolution and the origin of the skarn ore deposit. Ore Geol Rev 35:401–414

National Iranian Copper Industries Company (2008) Report of exploration study in Sonajil area

Niazi M, Asoudeh I (1978) The depth of seismicity in the Kermanshah region of the Zagros Mountains (Iran). Earth and Planetary Science Letter 40:270–274

Panahi A, Cheng Q, Bonham-Carter F (2004) Modelling lake sediment geochemical distribution using principal component, indicator kriging and multifractal power-spectrum analysis: a case study from Gowganda, Ontario. Geochemistry: Exploration, Environment, Analysis 4:59–70

Pourhosseini F (1981) Petrogenesis of Iranian plutons: a study of the Natanz and Bazman intrusive complexes: Ph.D. thesis, University of Cambridge, 315 pp.

Shahabpour J (1994) Post mineralization breccias dike from the Sarcheshmeh porphyry copper porphyry system. Kerman, Iran: Exploration and Mining geology 3:39–43

Sillitoe RH (1995) Exploration and discovery if base- and precious-metal deposits in the circum-Pacific region during the last 25 years. Metal Mining Agency of Japan

Spitz G, Darling R (1978) Major and minor element lithogeochemical anomalies surrounding 508 the Louvem copper deposit, Val d'Or, Québec. Canadian Journal of Earth Sciences 15(7):1161–1169

Stocklin J (1977) Structural correlation of the Alpine ranges between Iran and Central Asia. Mem. H. Aser. Soc. Geol. France, pp. 333–353

Waterman GC, Hamilton RL (1975) The Sarcheshmeh porphyry copper porphyry system. Econimic Geology 70:568–576

Yoshihiro U (2009) Relationship between statistical thermal alteration index and vitrinite reflectance for sedimentary rocks in northern Japan with reference to effects for unconformity, faulting, and contact metamorphism. Island Arc 18:661–668, Geological Society of Japan